Surface & Coatings Technology 320 (2017) 298–303

Contents lists available at ScienceDirect

Surface & Coatings Technology

journal homepage: www.elsevier.com/locate/surfcoat

Improved surface quality of layered architecture TiAlTaN/Ta coatings for high precision micromachining

Xudong Sui, Guojian Li *, Chenjie Jiang, Yang Gao, Kai Wang, Qiang Wang

Key Laboratory of Electromagnetic Processing of Materials (Ministry of Education), Northeastern University, Shenyang 110004, China

ARTICLE INFO

Article history:
Received 2 August 2016
Revised 25 November 2016
Accepted in revised form 21 December 2016
Available online 22 December 2016

Keywords:
Layered design
TiAlTaN
Micromachining
Surface roughness
Friction

ABSTRACT

High surface quality coatings play an important role in producing high precision coating tools for micromachining. This study focuses on the improvement of the coating surface quality by layered design method. The layered TiAlTaN/Ta coatings have been prepared by magnetron sputtering. SEM and AFM results revealed that the continuous growth of the columnar TiAlTaN crystals can be interrupted by layered design. The columnar crystal size of TiAlTaN coating decreased with the decreasing bilayer thickness. The coating surface roughness also gradually decreased from 36.6 ± 1.2 to 11.54 ± 0.6 to 8.9 ± 0.1 nm. Nanoidentation results showed an increasing coating hardness from 16 GPa to 20 GPa with decreasing bilayer thickness. Friction and wear test revealed that the coating friction coefficient increases from 0.70 to 0.93, then decreases to 0.62 with decreasing bilayer thickness. The layered method can improve mechanical and friction properties, meanwhile reducing surface roughness, which makes it a potentially promising method for fabricating high precision micromachining coating tools.

1. Introduction

Micromachining has been widely applied in the production of complex 3D parts such as MEMS parts, microlens arrays, bio-medical devices and various aerospace components [1–3]. The performance of these precision parts has a great sensitive to their surface quality and geometric errors [4–5]. In the process, the precision and quality can be significantly affected by the geometric precision of cutting edge and coating [6–8]. For example, the surface roughness of the workpiece can be affected directly by the geometric precision of coating tools [9]. Even if the tool substrate can be treated to a very high dimensional accuracy, it will lose its precision by following conventional coating process, such as arc ion plating. The limited precision and surface quality of traditional plating coating tool can lead to the onset of dynamic stability and chatter which can result in poor surface finish and even catastrophic tool failure [10]. Therefore, an ion plating apparatus with magnetic filter device is usually used to solve the problem of large particles [11]. Furthermore, post-treatment processes such as polishing are also used to improve the surface quality of the coating [12]. However, the high cost and low efficiency limit the application of these methods.

In recent years, biological design methods have found their way into hard coating industry. Layered design method is one of the successful biological designs, and acts as possible candidates for coatings to achieve numerous excellent properties [13–16]. However, extensive researches have focused on the improvement of the strength and fracture toughness caused by layered design [17–21]. The crystal growth and surface morphology in the layered coating has not gained much attention so far. The layered design can change the crystal growth and affect the coating surface morphology and roughness. Meanwhile, it does not need additional post-treatment. So the layered design is suitable for fabricating the hard coatings in high precision micromachining field.

Previous studies have shown that TiAlTaN coating exhibits excellent oxidation resistance and mechanical properties in the fields of high speed cutting and dry cutting [22,23]. The tribological properties at high temperature of over 900 °C can be enhanced by doping Ta in the coating [24]. Furthermore, the multilayer structure of pure Ta coating and TiAlTaN coating induces the formation of TaO lubricious oxide. This leads to a low friction coefficient and also reduction of the adhesion between tool coating and workpiece [25]. In addition, the sputtering coatings usually have good surface quality, which makes them suitable for using in high-precision coating tools. However, the structure of a sputtering coating is usually not dense and is easy to form coarse columnar crystal due to the low energy of deposited particles [26]. The application of layered design into sputtering coatings is an effect method to solve above problem.

Therefore, the TiAlTaN/Ta coatings were prepared by magnetron sputtering method in this study. The effects of layered structure on the

* Corresponding author.
E-mail address: gjli@epm.neu.edu.cn (G. Li).

http://dx.doi.org/10.1016/j.surfcoat.2016.12.083
0257-8972/

crystal growth, morphology, surface roughness, friction and mechanical properties in the TiAlTaN/Ta coatings were investigated.

2. Experimental details

TiAlTaN/Ta layered coatings were prepared on cemented carbide (YG8, Co = 8 wt.%) substrate using reactive magnetron sputtering method. The magnetron sputtering device equipped with four 3.5-inch targets. The substrates were first ground with diamond abrasive discs, and then polished with diamond pastes of 2.5 and 0.5 μm respectively, until smooth surfaces with a roughness of Sq ≈ 10 nm were obtained. Then, substrates were cleaned with acetone and ethanol in an ultrasonic cleaner, respectively. The details of pre-treatment method are identical to our previous report [27].

After the base pressure reached to 3×10^{-3} Pa, the substrate was heated up to 400 °C. Pure Ta target (99.99%) and $Ti_{0.50}Al_{0.50}$ alloy target (99.9%) were driven by RF and DC power respectively. All targets were cleaned by sputtering in pure argon gas for 5 min before depositing the coatings. Ti buffer layer was first deposited in an argon pressure of 0.5 Pa for 5 min. Then the total work pressure were maintained at 0.5 Pa with $P_{N2}/(P_{Ar} + P_{N2}) = 30\%$. The TiAlTaN layer was deposited with the Ta target power of 300 W and $Ti_{0.50}Al_{0.50}$ target power of 900 W. After TiAlTaN layer deposition was completed, the N_2 flow was closed. A pure Ar gas was fed to the chamber at a pressure of 0.5 Pa. The Ta target was operated at 300 W to obtain Ta layer. The TiAlTaN and Ta layer were deposited alternately. And the thickness of each layer was tuned by controlling the deposition time. The obtained coatings with different bilayer thickness are defined as TiAlTaN monolayer, TiAlTaN/Ta-1000 and TiAlTaN/Ta-140, where the number 1000 and 140 nm represents the thickness of the bilayer thickness in this work.

The morphology and thickness of the coatings were characterized by a scanning electron microscope (SEM, SUPRA 35). The attached energy dispersive spectrometer (EDS, OXFORD) was used for evaluating the chemical composition. The coating surface roughness was determined with an atomic force microscope (AFM, NANOSURF C3000). The friction and scratch tests were all conducted on a multi-functional tester for materials surface properties (MFT-4001). The load force and friction speed is 5 N and 100 mm/min respectively in the friction test. To simulate the friction between coating and titanium, a Ti6Al4V ball (φ6 mm) was used as friction counterpart. The scratch test was conducted with a loading rate of 100 N/min and a scratch length of 5 mm.

3. Results and discussion

3.1. Coating structure and morphology

The cross-section morphology of TiAlTaN and TiAlTaN/Ta coatings are observed by SEM, as shown in Fig. 1. At the early stage of growth (zone A), the TiAlTaN coating exhibits a fine-grain structure and evolves into columnar structure. The columnar diameter gradually increases as the coating grows and remains unchanged when the coating grows past one-half of the coating thickness in zone B. However, this continuous columnar growth was interrupted by inserting Ta layer. The TiAlTaN/Ta-1000 coating has a smaller columnar diameter and becomes more compact in Zone C compared with the results of TiAlTaN coating. This is because columnar crystal in layered coatings needs re-nucleation and growth on the interface [28,29] due to the different lattice constants between TiAlTaN (a ≈ 0.424 nm) and Ta (a ≈ 0.331 nm). In addition, the columnar diameter is reduced by decreasing bilayer thickness from 1000 to 140 nm. The columnar crystal in TiAlTaN/Ta-140 coating seems to become fine-grain structure. This is because the columnar crystals are easy to be suppressed by introducing Ta layer under a small bilayer thickness, as shown in zone D in Fig. 1.

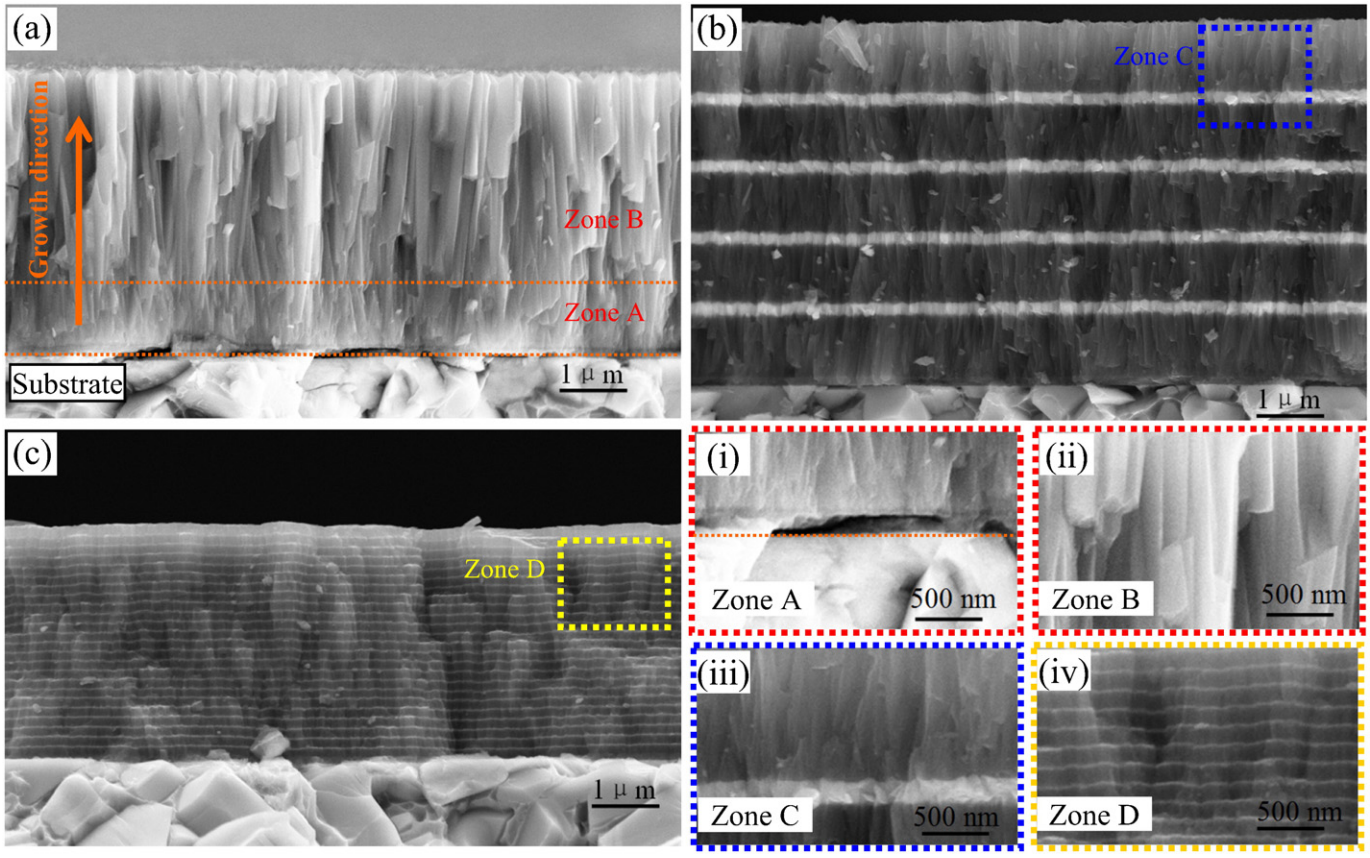

Fig. 1. Cross-section SEM images of coatings of (a) TiAlTaN, (b) TiAlTaN/Ta-1000, and (c) TiAlTaN/Ta-140. The insets (i) to (iv) are the corresponding enlarge views of TiAlTaN, TiAlTaN/Ta-1000 and TiAlTaN/Ta-140, respectively.

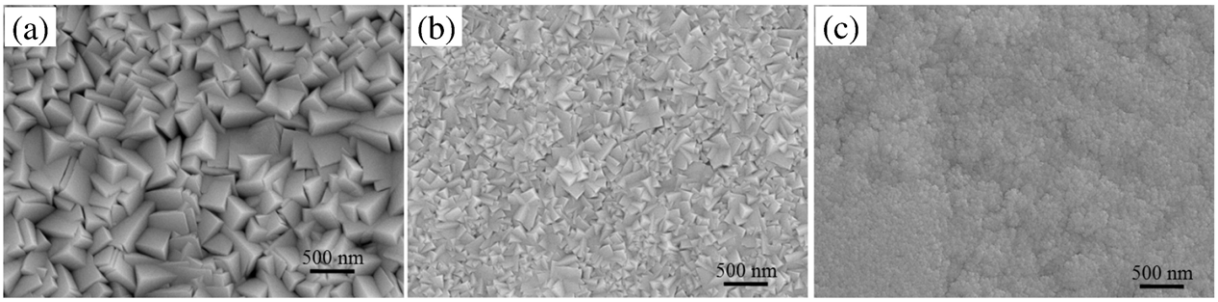

Fig. 2. SEM images of coatings of (a) TiAlTaN, (b) TiAlTaN/Ta-1000, and (c) TiAlTaN/Ta-140.

The coating surface morphologies are shown in Fig. 2. It can be found that the TiAlTaN coating shows well-faced crystal morphology with sharp pyramidal structures (Fig. 2(a)) because of well developed large columnar crystal in the coating. The well-faced morphology is blunted and becomes rounded morphology for the TiAlTaN/Ta-1000 coating. Moreover, the particle size decreases with decreasing bilayer thickness and the trend is consistent with the change of columnar diameter. This morphology change can decrease the surface roughness of the layered coatings.

The surface roughness of these three kinds of coatings characterized by AFM is shown in Fig. 3. The surface roughness (Sq = 36.6 nm) of TiAlTaN coating was sharply decreased by comparing with the layered coatings. The surface roughness decreases from 11.54 ± 0.6 to 8.9 ± 0.1 nm as the decrease of the bilayer thickness. The surface roughness of the TiAlTaN/Ta-140 coating is smaller than that of the substrate. This means that additional tolerance was not introduced into a high precision tool in the layered coating. In addition, the coating line roughness agrees well with the results of the surface roughness as shown in the bottom of Fig. 3.

The results of decreasing in roughness with the bilayer thickness in Fig. 3 are consistent with the SEM results. There are two reasons contributed to this phenomenon according to previous studies [30–32]. One is the re-nucleation of crystals. As described above, the Ta and TiAlTaN layers were significantly different in structure and composition. This would lead to a re-nucleation on the interface of each deposited layers, and ultimately produce a smoother surface as shown in Fig. 2. The other is the interface energy of the coatings. As the bilayer thickness decreases, the interface number in coatings increases. This would lead to increased interface energy at smaller bilayer thickness. Since the curved particle surface can minimize the total surface energy, the well-faced pyramidal surface (Fig. 2(a)) would changes to a more rounded or curved surface (Fig. 2(c)) with the decreasing bilayer thickness. Therefore, these two factors are conducive to reducing the coating roughness with the decreasing bilayer thickness.

3.2. Hardness and adherence force

The hardness of all the coatings is shown in Fig. 4. The coating hardness increases from 16 GPa to 20 GPa with decreasing the bilayer thickness. The TiAlTaN/Ta-140 has the highest hardness (about 20 GPa). This mainly attributes to the decrease of the columnar diameter in the layered coating according to the Hall-Petch formula [13,33]. In addition, the increasing amount of interfaces in the layered coatings can inhibit dislocation and extension of cracks [13,34]. This increases the hardness of TiAlTaN/Ta layered coatings.

The results of the scratch test are shown in Fig. 5. The minimum critical loads of all coatings are > 70 N. The good adhesion is related with the presence of Ti buffer layer [35]. It can be found that the critical load of

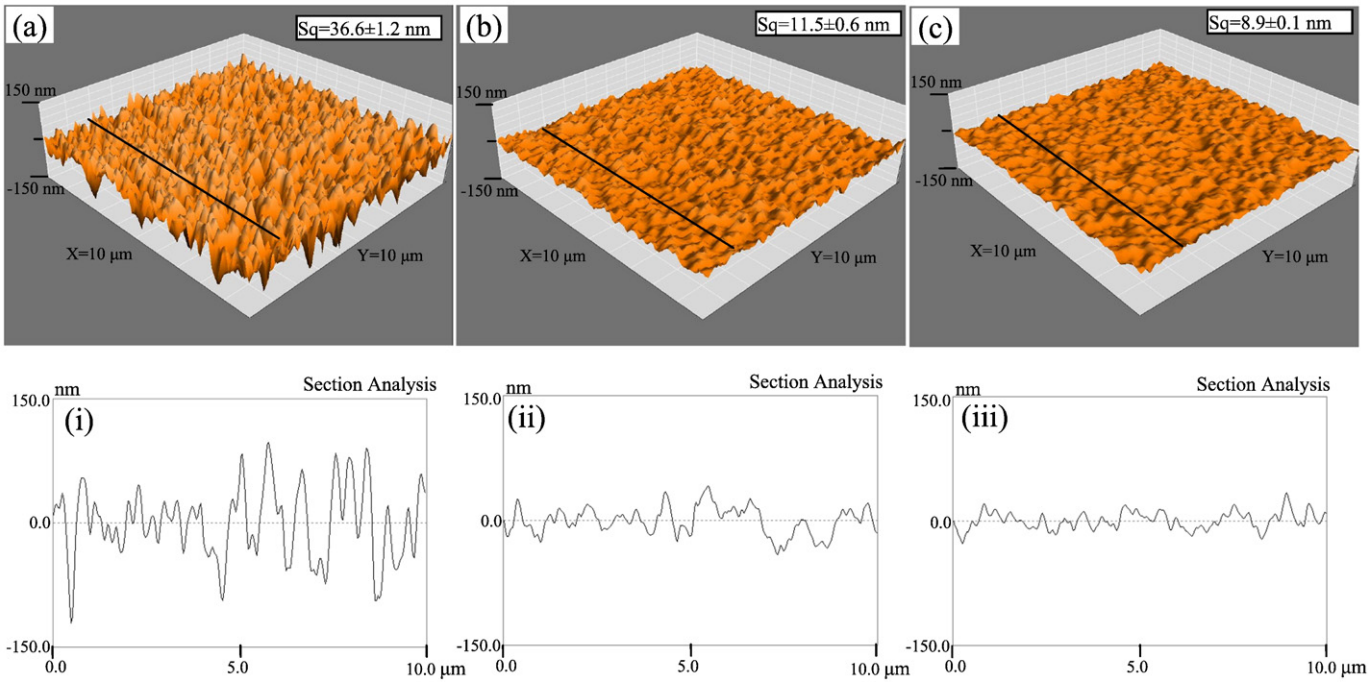

Fig. 3. AFM images of coatings of (a) TiAlTaN, (b) TiAlTaN/Ta-1000, and (c) TiAlTaN/Ta-140. The insets (i), (ii) and (iii) are the corresponding line roughness curves of TiAlTaN, TiAlTaN/Ta-1000, and TiAlTaN/Ta-140, respectively.

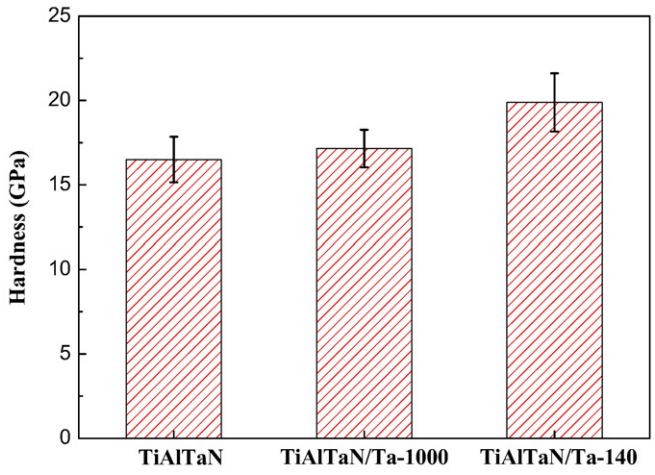

Fig. 4. Nanoindentation results of coatings of (a) TiAlTaN, (b) TiAlTaN/Ta-1000, and (c) TiAlTaN/Ta-140.

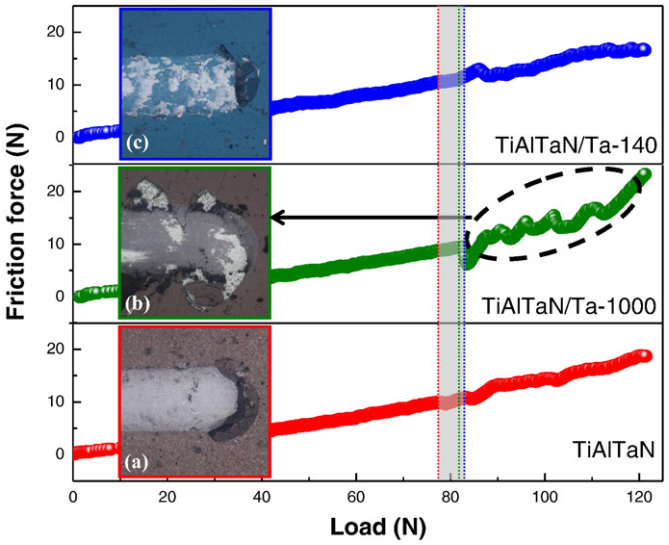

Fig. 6. Friction force and scratch morphology of coatings of (a) TiAlTaN, (b) TiAlTaN/Ta-1000, and (c) TiAlTaN/Ta-140.

layered coating is slightly higher than that of the TiAlTaN coating. This is mainly due to the small surface roughness and strong crack inhibition caused by layered structure.

The friction force during scratch test is also measured as shown in Fig. 6. It can be observed that the friction forces increase linearly with the loading force, and have an abrupt change around 85 N as shown by gray area in Fig. 6. This is consistent with the acoustic emission results. However, the friction force of TiAlTaN/Ta-1000 coating fluctuates greatly at the end of scratch test as shown by the dashed cycle in Fig. 6. This is because that the diamond indenter has a different friction environment in the Ta and TiAlTaN layer. Since the relative poor adhesion between the Ta and TiAlTaN layer, the deep transverse cracks and chipping occur on both edges of the scratch track, as seen in inserts (b) of Fig. 6. These problems can be improved by decreasing the bilayer thickness. With the bilayer thickness decrease from 1000 nm to 140 nm, the Ta layer thickness decreases from 180 nm to 25 nm. The friction fluctuation and chipping in the TiAlTaN/Ta-140 coating disappears as shown in Fig. 6.

3.3. Friction and wear mechanism

Friction properties of the coating tools play a key role to the cutting performance in micro-machining application. High friction coefficient increases the frictional heat and cutting force, which will reduce machining accuracy and tool life. In this work, the Ti6Al4V ball is chosen to compose the friction counterpart with the coatings. This is because Ti6Al4V alloy has been widely used to manufacture various precision complex 3D parts in aerospace and bio-medical fields. Adhesive wear is one of the most critical issues during machining this alloy. Previous studies show that low friction coefficient can reduce adhesive wear [6–8,12]. Therefore, it is important to measure the friction and wear test of the TiAlTaN and TiAlTaN/Ta layered coatings.

The obtained friction and wear curve of coatings is presented in Fig. 7. The dashed lines in Fig. 7 represent the average friction coefficient after the friction test reached steady state. The friction coefficients of TiAlTaN, TiAlTaN/Ta-1000 and TiAlTaN/Ta-140 coatings are 0.70, 0.93 and 0.62 respectively. The thickness of Ta layer has an effect on the friction coefficient of layered coatings. When the thickness of Ta layer is too thick, it is easy to cause the coating to peel off (Fig. 6(b)). The excessive wear debris can deteriorate friction environment, leading to increase the friction coefficient. With the bilayer thickness decrease from 1000 nm to 140 nm, the Ta layer thickness decreases from 180 nm to 25 nm. The above chipping problems can be effectively improved as shown in Fig. 6(c). Moreover, the TiAlTaN/Ta-140 coating has the lowest surface roughness. All these factors make TiAlTaN/Ta-140 coating obtaining the lowest friction coefficient.

The wear tracks of the coatings are characterized by SEM and EDS to investigate the wear mechanism, as shown in Fig. 8 and Table 1. The yellow strip at the right of Fig. 8 represents the wear track of coatings after

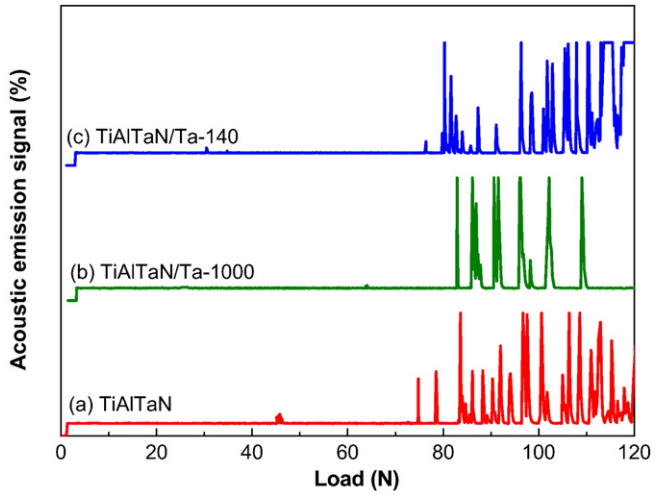

Fig. 5. Acoustic emission curves of coatings of (a) TiAlTaN, (b) TiAlTaN/Ta-1000, and (c) TiAlTaN/Ta-140.

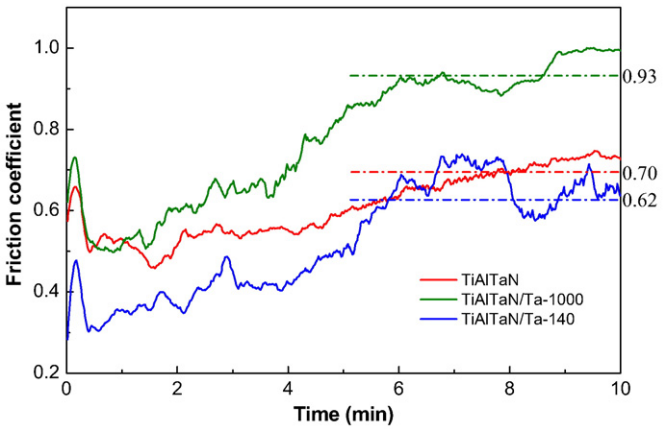

Fig. 7. Friction coefficients of coatings: (a) TiAlTaN, (b) TiAlTaN/Ta-1000, (c) TiAlTaN/Ta-140.

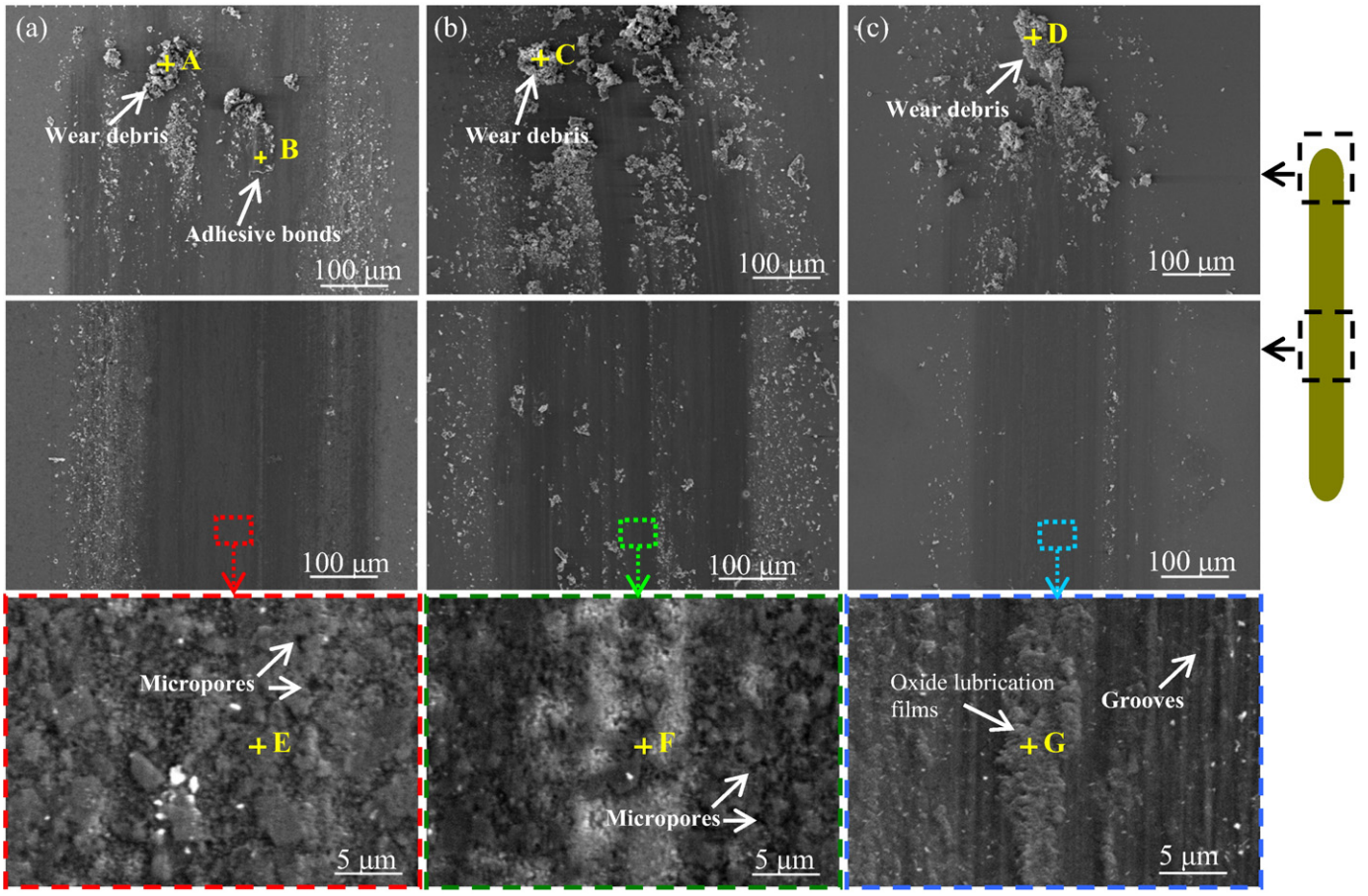

Fig. 8. SEM images of the wear tracks of coatings of (a) TiAlTaN, (b) TiAlTaN/Ta-1000, and (c) TiAlTaN/Ta-140. The top images show the morphologies at the end of wear tracks of the coatings. The middle images show the morphologies at the middle of wear tracks of the coatings. The bottom images are the enlarge view of select area in the centre of the wear tracks.

a reciprocating friction and wear test. It can be found that the wear debris appears along the wear edge of all the coatings. EDS results (point A, C and D) show that the compositions of debris mainly include Ti, Al, Ta and O and are close to those of the coatings. There are some adhesive bonds on the TiAlTaN coating (Fig. 8(a)). EDS result of point B shows that they are Ti, Al, V and O. The element V can only come from the Ti6Al4V counterpart. This means that adhesive phenomenon between titanium and coating occurs. The wear track of the TiAlTaN coating has many micropores and exhibits an uneven, discontinuous and island morphology as shown in the bottom image of Fig. 8(a). This is because the large particle size and rough surface of TiAlTaN coating. EDS results show that the wear track of TiAlTaN coating mainly contains Ti, Al, V and O. Thus, the wear mechanism of TiAlTaN coating is a mixture of adhesive wear and oxidation wear. As the bilayer thickness decreases, this uneven and discontinuous island wear morphology becomes more continuous and smoother (the bottom image of Fig. 8(c)). This is mainly caused by two reasons. One reason is the small particle size and surface roughness in the layered coatings with a low bilayer thickness. The other reason is the formation of the oxide lubrication films (such as TaO, Al_2O_3 and so on). This can be proved by EDS results (point E, F and G in Fig. 8). The existence of these lubrication films can reduce friction coefficient and adhesive wear. In the ensuing friction, these oxides and the debris can form micro-asperities in sliding area and act as scratch indenters under the action of vertical acting load. As a result, the grooves are formed [36]. Therefore, the wear mechanism of TiAlTaN/Ta-140 coating is oxidation wear and groove wear.

Table 1
EDS results of different coatings after friction experiments.

Point	Ti (at.%)	Al (at.%)	Ta (at.%)	V (at.%)	N (at.%)	O (at.%)
A	28.29	5.37	–	–	–	66.34
B	50.44	10.99	–	2.84	–	35.73
C	22.18	3.92	–	0.85	–	73.05
D	13.73	4.58	2.26	–	–	79.43
E	31.54	5.98	–	1.59	–	60.89
F	11.35	19.50	2.84	–	51.15	15.17
G	10.35	15.80	2.53	–	29.20	42.11

4. Conclusions

The layered TiAlTaN/Ta composite coatings with different bilayer thickness have been fabricated by using magnetic sputtering method. The coating structure and morphology were evaluated by SEM and AFM. The results revealed that the continuous growth of columnar crystals can be interrupted by layered design. The columnar crystal size of TiAlTaN layer decreased with the decreasing bilayer thickness. The coating surface roughness also gradually decreased from 36.6 ± 1.2 to 11.54 ± 0.6 to 8.9 ± 0.1 nm. The lowest surface roughness obtained in TiAlTaN/Ta-140 coating was superior to that of polished substrate, which means it would not introduce additional tolerance into a high precision tool substrate after coating process. Nanoidentation results showed that the coating hardness increases with the decreasing bilayer thickness. The friction and wear test revealed that the coating friction coefficient increases from 0.70 to 0.93, then decrease to 0.62 with the decrease of bilayer thickness. The layered design of alternative depositing TiAlTaN and Ta layers reduced adhesive wear between coatings and titanium counterpart.

Therefore, the layered design method can be used to improve the surface roughness and hardness while reducing the friction coefficient and adhesive wear. This method can be expected to replace the post-

treatment process or further improve the surface quality of the high precision micromachining coating tools.

Acknowledgments

The authors gratefully acknowledge the financial support of the National Science and Technology Major Project (2012ZX04003061).

References

[1] J.C. Miao, G.L. Chen, X.M. Lai, H.T. Li, C.F. Li, Review of dynamic issue in micro-end-milling, Int. J. Adv. Manuf. Technol. 31 (2007) 897–904.
[2] X.L. Liu, X.D. Zhang, F.Z. Fang, Z. Zeng, H.M. Gao, X.T. Hu, Influence of machining errors on form errors of microlens arrays in ultra-precision turning, Int. J. Mach. Tools Manuf. 96 (2015) 80–93.
[3] W. Li, Z.X. Zhou, X.M. Huang, Z.J. He, Y. Du, Development of a high-speed and precision micro-spindle for micro-cutting, Int. J. Precis. Eng. Manuf. 15 (2014) 2375–2383.
[4] C.H. Lauro, L.C. Brandao, T.H. Panzera, J.P. Davim, Surface integrity in the micromachining: a review, Rev. Adv. Mater. Sci. 40 (2015) 227–234.
[5] J. Šícha, D. Heřman, J. Musil, Z. Strýhal, J. Pavlík, Surface morphology of magnetron sputtered TiO_2 films, Plasma Process. Polym. 4 (2007) 345–349.
[6] Y.X. Qiu, S. Zhang, J.W. Lee, B. Li, Y.X. Wang, D.L. Zhao, Self-lubricating CrAlN/VN multilayer coatings at room temperature, Appl. Surf. Sci. 279 (2013) 189–196.
[7] S.M. Aouadi, H. Gao, A. Martini, T.W. Scharf, C. Muratore, Lubricious oxide coatings for extreme temperature applications: a review, Surf. Coat. Technol. 257 (2014) 266–277.
[8] T. Wang, G.J. Zhang, B.L. Jiang, Microstructure, mechanical and tribological properties of TiMoN/Si_3N_4 nano-multilayer films deposited by magnetron sputtering, Appl. Surf. Sci. 326 (2015) 162–167.
[9] T. Altan, B. Lilly, Y.C. Yen, Manufacturing of dies and moulds, CIRP Ann. Manuf. Technol. 50 (2001) 404.
[10] K.K. Singh, V. Kartik, R. Singh, Modeling dynamic stability in high-speed micromilling of Ti–6Al–4V via velocity and chip load dependent cutting coefficients, Int. J. Mach. Tools Manuf. 96 (2015) 56–66.
[11] L. Han, L. Yang, L.M.C. Yang, Y.W. Wang, Y.Q. Zhao, Effect of magnetic filtering coil current on the tribology property of tetrahedral amorphous carbon films, Acta. Phys. Sin. 60 (2011) 046802.
[12] H. Yamaguchi, A.K. Srivastava, M.A. Tan, Magnetic abrasive finishing of cutting tools for machining of titanium alloys, CIRP. Ann. Manuf. Technol. 61 (2012) 311–314.
[13] P.C. Yashar, W.D. Sproul, Nanometer scale multilayered hard coatings, Vacuum 55 (1999) 179–190.
[14] P. Angerer, J.M. Lackner, M. Wiessner, G.A. Maier, L. Major, Thermal behaviour of chromium nitride/titanium–titanium carbonitride multilayers, Thin Solid Films 562 (2014) 159–165.
[15] J. Romero, A. Lousa, E. Martinez, J. Esteve, Nanometric chromium/chromium carbide multilayers for tribological applications, Surf. Coat. Technol. 163-164 (2003) 392.
[16] P. Li, L. Chen, S.Q. Wang, B. Yang, Y. Du, J. Li, M.J. Wu, Microstructure, mechanical and thermal properties of TiAlN/CrAlN multilayer coatings, Int. J. Refract. Met. Hard Mater. 40 (2013) 51–57.
[17] J.Y. Zhang, G. Liu, X. Zhang, G.J. Zhang, J. Sun, E. Ma, A maximum in ductility and fracture toughness in nanostructured Cu/Cr multilayer films, Scr. Mater. 62 (2010) 333–336.
[18] S. Kaciulis, A. Mezzi, G. Montesperelli, F. Lamastra, M. Rapone, F. Casadei, T. Valente, G. Gusmano, Multi-technique study of corrosion resistant CrN/Cr/CrN and CrN: C coatings, Surf. Coat. Technol. 201 (2006) 313–319.
[19] M.B. Daia, P. Aubert, S. Labdi, C. Sant, F.A. Sadi, P. Houdy, J.L. Bozet, Nanoinden-tation investigation of Ti/TiN multilayers films, J. Appl. Phys. 87 (11) (2000) 7753–7757.
[20] J.H. Lee, W.M. Kim, T.S. Lee, M.K. Chung, B.K. Cheong, S.G. Kim, Mechanical and adhesion properties of Al/AlN multilayered thin films, Surf. Coat. Technol. 220 (2000) 133–134.
[21] S. Zhang, H.L. Wang, S.E. Ong, D. Sun, X.L. Bui, Hard yet tough nanocomposite coatings-present status and future trends, Plasma Process. Polym. 4 (2007) 219–228.
[22] R. Rachbauer, D. Holec, P.H. Mayrhofer, Increase thermal stability of Ti-Al-N thin films by Ta alloying, Surf. Coat. Technol. 211 (2012) 98–103.
[23] R. Hollerweger, H. Riedl, J. Paulitsch, M. Arndt, R. Rachbauer, P. Polcik, S. Primig, P.H. Mayrhofer, Origin of high temperature oxidation resistance of Ti-Al-Ta-N coatings, Surf. Coat. Technol. 257 (2014) 78–86.
[24] M. Pfeiler, G.A. Fontalvo, J. Wagner, K. Kutschej, M. Penoy, C. Michotte, C. Mit-terer, M. Kathrein, Arc evaporation of Ti-Al-Ta-N coatings: the effect of bias voltage and Ta on high-temperature tribological properties, Tribol. Lett. 30 (2008) 91–97.
[25] G.J. Li, X.D. Sui, C.J. Jiang, Y. Gao, K. Wang, Q. Wang, D. Liu, Low adhesion effect of TiAlTaN/TaO functional composite coatings on the titanium cutting performance of coated cemented carbide inserts, Mater. Des. 110 (2016) 105–111.
[26] L. Chen, K.K. Chang, Y. Du, J.R. Li, M.J. Wu, A comparative research on magnetron sputtering and arc evaporation deposition of Ti-Al-N coatings, Thin Solid Films 519 (2011) 3762–3767.
[27] X.D. Sui, G.J. Li, X.S. Qin, H.D. Yu, Q. Wang, Relationship of microstructure, mechanical properties and titanium cutting performance of TiAlN/TiAlSiN composite coated tool, Ceram. Int. 42 (2016) 7524–7532.
[28] K. Kaouther, D. Hafedh, Z. Lassaad, B.C.L. Ahmed, Mechanical characterization of CrN/CrAlN multilayer coatings deposited by magnetron sputtering system, J. Mater. Eng. Perform. 24 (2015) 4077–4082.
[29] A. Zeilinger, R. Daniel, M. Stefenelli, B. Sartory, L. Chitu, M. Burghammer, T. Schöberl, O. Kolednik, J. Keckes, C. Mitterer, Mechanical property enhancement in laminates through control of morphology and crystal orientation, J. Phys. D. Appl. Phys. 48 (2015) 295303.
[30] K. Chu, Y.G. Shen, Mechanical and tribological characterisation of nanostructured Ti/TiB_2 multilayer films, Surf. Eng. 24 (2008) 402–409.
[31] J. Xu, K. Hattori, Y. Seino, I. Kojima, Microstructure and properties of CrN/Si_3N_4 nanostructured multilayer films, Thin Solid Films 414 (2002) 239–245.
[32] D.A. Delisle, J.E. Krzanowski, Surface morphology and texture of TiAlN/CrN multilayer coatings, Thin Solid Films 524 (2012) 100–106.
[33] U. Helmersson, S. Todorova, S.A. Barnett, J.E. Sundgren, L. Markert, J.E. Greene, Growth of single-crystal TiN/VN strained-layer superlattice with extremely high mechanical hardness, J. Appl. Phys. 62 (1987) 481–484.
[34] J. Musil, Hard and superhard nanocomposite coatings, Surf. Coat. Technol. 125 (2000) 322–330.
[35] G.S. Kim, S.Y. Lee, J.H. Hahn, B.Y. Lee, J.G. Han, J.H. Lee, S.Y. Lee, Effects of the thickness of Ti buffer layer on the mechanical properties of TiN coatings, Surf. Coat. Technol. 171 (2003) 83–90.
[36] A.H. Liu, J.X. Deng, H.B. Cui, Y.Y. Chen, J. Zhao, Friction and wear properties of TiN, TiAlN, AlTiN and CrAlN PVD nitride coatings, Int. J. Refract. Met. Hard Mater. 31 (2012) 82–88.